



저작자표시-비영리-변경금지 2.0 대한민국

이용자는 아래의 조건을 따르는 경우에 한하여 자유롭게

- 이 저작물을 복제, 배포, 전송, 전시, 공연 및 방송할 수 있습니다.

다음과 같은 조건을 따라야 합니다:



저작자표시. 귀하는 원저작자를 표시하여야 합니다.



비영리. 귀하는 이 저작물을 영리 목적으로 이용할 수 없습니다.



변경금지. 귀하는 이 저작물을 개작, 변형 또는 가공할 수 없습니다.

- 귀하는, 이 저작물의 재이용이나 배포의 경우, 이 저작물에 적용된 이용허락조건을 명확하게 나타내어야 합니다.
- 저작권자로부터 별도의 허가를 받으면 이러한 조건들은 적용되지 않습니다.

저작권법에 따른 이용자의 권리는 위의 내용에 의하여 영향을 받지 않습니다.

이것은 [이용허락규약\(Legal Code\)](#)을 이해하기 쉽게 요약한 것입니다.

[Disclaimer](#)

**Photo-crosslinked gelatin methacryloyl hydrogel
strengthened with calcium phosphate-based nanoparticles
by different methods for early healing of rabbit calvarial
defects**

Da-Na Lee

Department of Dentistry

The Graduate School, Yonsei University

**Photo-crosslinked gelatin methacryloyl hydrogel
strengthened with calcium phosphate-based nanoparticles
by different methods for early healing of rabbit calvarial
defects**


Directed by Professor Seong-Ho Choi

The Doctoral Dissertation
submitted to the Department of Dentistry
and the Graduate School of Yonsei University
in partial fulfillment of the requirements for the degree of
Ph.D. in Dental Science

Da-Na Lee

December 2022


This certifies that the Doctoral Dissertation
of Da-Na Lee is approved.



Thesis Supervisor: Seong-Ho Choi



Ui-Won Jung



Jung-Seok Lee



Jae-Kook Cha



Jeong-Won Paik

The Graduate School
Yonsei University
December 2022

감사의 글

제일 먼저, 본 연구가 완성 되기까지 부족한 저를 이끌어주시고, 사랑과 격려로 가르침 주신 최성호 교수님께 진심으로 감사드립니다. 교수님의 제자로 치주과에서 수련 받을 수 있어 영광이었습니다. 연구진행 시작부터 마무리 될 때까지 심혈을 기울여 주시고, 아낌없는 조언을 해주신 박진영 교수님께도 깊이 감사드립니다. 아울러 저의 학위 논문 심사를 맡아 주시고, 치주과 의사로 성장할 수 있도록 지도해주신 김창성, 정의원, 이중석, 차재국, 백정원, 송영우 교수님께 감사의 마음을 전합니다.

그리고 연구를 진행하는데 많은 도움을 준 연구원 선생님들, 함께 공부하며 버팀목이 되어준 치주과 동기들, 의국 선후배들에게도 감사드립니다.

마지막으로 넘치는 사랑과 기도로 묵묵히 저를 응원해주시고, 격려해주신 아빠, 엄마, 존재만으로도 큰 힘이 되는 언니, 매일 아침 손녀를 위해 기도해주시는 할아버지, 할머니 사랑과 감사의 마음을 전합니다.

2022년 12월

저자 이다나

TABLE OF CONTENTS

List of figures	iii
List of tables	iv
Abstract (English)	v
I. INTRODUCTION	1
II. MATERIALS AND METHODS	4
1. Experimental animals	4
2. Preparation of GelMa	4
3. Scanning Electron Microscope (SEM) analysis	5
4. Study design	5
5. Sample size determination	6
6. Surgical procedure	6
7. Micro-CT analysis	7
8. Histologic and histomorphometric analyses	8
9. Statistical analysis	8
III. RESULTS	9
1. Clinical observations	9

2. Scanning Electron Microscope (SEM) analysis	9
3. Micro-CT analysis	9
4. Histologic observations	10
5. Histomorphometric analysis	11
IV. DISCUSSION	12
V. CONCLUSION	16
Reference	17
Tables	22
Figures	25
Abstract (Korean)	34

List of figures

Figure 1. Clinical photograph of samples.

Figure 2. Experimental design in the rabbit calvarium.

Figure 3. Microstructure surface images of samples using scanning electron microscopy (15.0 kV).

Figure 4. Three-dimensionally reconstructed micro-computed tomography images of the rabbit calvaria at 2, 4 and 8 weeks.

Figure 5. The results from the volumetric analysis represented as graphs.

Figure 6. Histological view of each group at 2 weeks.

Figure 7. Histological view of each group at 4 weeks.

Figure 8. Histological view of each group at 8 weeks.

Figure 9. The results from the histomorphometric analysis represented as graphs.

List of tables

Table 1. The composition of different GelMa hydrogel samples.

Table 2. Volumetric results from the micro-CT analysis (mm^3).

Table 3. Results from the histomorphometric analysis (mm^2).

Abstract

**Photo-crosslinked gelatin methacryloyl hydrogel
strengthened with calcium phosphate-based nanoparticles
by different methods for early healing of rabbit calvarial
defects**

Da-Na Lee, B.S., D.M.D.

*Department of Dentistry
The Graduate School, Yonsei University*

(Directed by Professor Seong-Ho Choi, D.D.S., M.S.D., PhD.)

Purpose: The aim of this study was to investigate the efficacy of photo-crosslinked gelatin methacryloyl (GelMa) hydrogel and calcium phosphate nanoparticles (CNp) when applying different fabrication methods for bone regeneration.

Methods: Four circular defects were created in the calvaria of 10 rabbits. Each defect was randomly allocated to the following study groups: 1) The sham control group; 2) The GelMa group (defect filled with crosslinked GelMa hydrogel); 3) The CNp-GelMa group (GelMa hydrogel crosslinked with nanoparticles); 4) The CNp+GelMa group (crosslinked

GelMa loaded with nanoparticles). At two, four and eight weeks, samples were harvested, and histological and micro-computed tomography analyses were performed.

Results: Histomorphometric analysis showed that CNp-GelMa and CNp+GelMa groups at 2 weeks were significantly greater in total augmented area compared to the control group ($P<0.05$). Greatest new bone area was observed in the CNp-GelMa group, however this was without statistical significance ($P>0.05$). Crosslinked GelMa hydrogel with nanoparticles exhibited good biocompatibility with minimal inflammatory reaction.

Conclusion: There was no difference in the efficacy of bone regeneration according to the synthesized method of photo-crosslinked GelMa hydrogel with nanoparticles. However, these materials could remain within a bone defect up to 2 weeks and showed good biocompatibility with little inflammatory response. Further improvement in mechanical properties and resistance to enzymatic degradation would be needed for the clinical application.

Keywords: Animals, biomaterials, bone regeneration, gelatin methacryloyl, nanoparticles,

**Photo-crosslinked gelatin methacryloyl hydrogel
strengthened with calcium phosphate-based nanoparticles
by different methods for early healing of rabbit calvarial
defects**

Da-Na Lee, B.S., D.M.D.

Department of Dentistry

The Graduate School, Yonsei University

(Directed by Professor Seong-Ho Choi, D.D.S., M.S.D., PhD.)

I. INTRODUCTION

The role of the scaffold in tissue engineering is to temporarily substitute the damaged tissue matrix during the regeneration process. The ideal characteristics of a scaffold materials include providing an environment for cell proliferation and functional differentiation, and mechanical support (Jiao et al., 2020). Various types of biomaterials have been investigated and developed in tissue engineering to potentially mimic the roles of extracellular matrix (ECM), which regulates tissue organization, cell behavior and allows the distribution of metabolites and growth factors(Lee and Mooney, 2001).

Hydrogels were widely studied as a scaffold due to their similar characteristics to the extracellular matrix (Serafim et al., 2014). Hydrogels, containing hydrophilic groups or domains with three-dimensional structure can be made from synthetic or natural polymers (Yue et al., 2015). Synthetic hydrogels such as poly(ethylene glycol) (PEG), poly(vinyl alcohol) (PVA), and poly(2-hydroxyethyl methacrylate) (PHEMA) hydrogels have the advantages of controllable degradation rate and modifiable mechanical strength (Annabi et al., 2010; Li et al., 2012). On the other hand, naturally derived hydrogels such as collagen, gelatin and hyaluronic acid have abilities of cell signaling, cellular interaction and biodegradability but can be limited by the low mechanical strength and uncontrolled degradation (Li et al., 2012). Thus, combinations of synthetic and natural hydrogels have been attempted to complement the properties each other.

Gelatin methacryloyl (GelMa) has recently attracted attention as a versatile biomaterial in the field of bioprinting and biofabrication with functional bioinks (McBeth et al., 2017). It can be synthesized by the reaction of free hydroxyl and amine groups on gelatin with methacrylate anhydride, preserving arginine-glycine-aspartic acid (RGD), which promotes cell adhesion (Rahali et al., 2017) and matrix metalloproteinase (MMP), responsible for enzymatic cleavage (Xiao et al., 2019). Then, by given UV radiation and photoinitiator, the side groups of gelatin chains are polymerized to produce covalently crosslinked gelatin network, which enhances mechanical rigidity and stability (Van Den Bulcke et al., 2000). GelMa hydrogels generally contain less than 5% methacrylic anhydride (Liu and Chan-Park, 2010), which means that most of functional motifs of gelatin such as RGD and MMP don't react with methacrylic anhydride. Therefore, GelMa hydrogels can be produced and modified with other components while preserving the characteristic of cell attachment that RGD promotes (Rahali et al., 2017).

The properties of GelMa hydrogel such as hydration, mechanical strength and degradability can be modified to satisfy the requirements of tissue engineering application by addition of materials to the hydrogel. Whether these additive materials can improve the

mechanical properties of GelMa is still controversial; many studies have attempted to develop materials for further practical applications (Heo et al., 2014b; Wang et al., 2018). A previous study has shown that GelMa hydrogel loaded with nanoparticles, carbon nanotubes and graphene oxide to serve as a stem cell scaffold, was effective in increasing the stiffness (Wang et al., 2018). In addition, a combined in vitro and vivo study showed that a GelMa hydrogel scaffold containing gold nanoparticles significantly increased new bone formation (Heo et al., 2014b). The results showed that gold nanoparticles promote proliferation, differentiation, and alkaline phosphate activities of human adipose-derived stem cell (ADSCs) and stimulate new bone formation. Inspired by previous works, we modified the structure of GelMa hydrogel by adding calcium phosphate-based nanoparticles with our own different fabrication strategy to reinforce its mechanical strength. There have been numerous in vitro studies and meta-analysis to characterize the mechanical properties of GelMa hydrogel (Zhang et al., 2021). To the best of our knowledge, this was the first study to apply GelMa hydrogel loaded with nanoparticles in an in vivo model. We hypothesized that photo-crosslinked gelatin methacryloyl hydrogel with nanoparticles would enhance bone regeneration.

The aim of this study was to investigate the regenerative capacity of photo-crosslinked GelMa hydrogel reinforced with nanoparticles at the early phase of bone healing. Furthermore, biocompatibility of GelMa hydrogel and the degradation characteristic at each period were assessed.

II. MATERIALS AND METHODS

1. Experimental animals

Ten 8-week-old male New Zealand white rabbits (2.8-3.2kg) were used in this study. The sample size was determined in accordance with the guideline for minimizing the number of experimental animals, refining procedures for improving animal welfare and replacing the use of animals with alternative protocols (Kilkenny, Browne, Cuthi, Emerson, & Altman, 2012). The study received ethical approval from the Animal Institution Animal Care and Use Committee of Yonsei Medical Center, Seoul, South Korea (approval number 2020-0285). The animal management, preparation and surgical procedures were performed in a laboratory which was accredited by International Association for Assessment and Accreditation of Laboratory Animals.

2. Preparation of GelMa

Synthesis of gelatin methacryloyl (GelMa) has been described in detail in a previous study (Noh et al., 2019). In brief, pure gelatin methacryloyl (GelMa) were synthesized by adding gelatin isolated from bovine skin (Sigma Aldrich, USA) and methacrylic anhydride (Sigma Aldrich, USA) in alkaline condition. Then, the obtained compound was dialyzed in distilled water for 4 days and lyophilized to gain pure GelMa.

Nanoparticle reinforced GelMa (NP-GelMa) was synthesized using a patented technique (KR 10-2020-0096101, 2020 (Applied: 15 July 2020)). This is a one-pot synthesis technique to produce the nanocomposite hydrogel *in situ*. The detailed characterizations and its physical and biological properties as well as their detailed mechanisms have been communicated in a preceding study (Bhattacharyya et al., 2022). For NP-GelMa, CaCl₂ was dissolved in distilled water. Gelatin was added to it and stirred in oil bath at 50 °C at 400 rpm for 6 hours to dissolve completely under pH 8. Na₂HPO₄ was dissolved in distilled water separately and added with stirring for 2 hours. The

temperature was increased to 60 °C and stirring continued for 30 min. Methacrylic anhydride (Sigma Aldrich, USA) was added slowly drop by drop and stirring continued for 3hours. Phosphate buffered saline was added in the reaction flask and then it was cooled down and dialyzed in distilled water for 4 days. After dialysis, it was freeze-dried to obtain the nanoparticle reinforced GelMa. Table 1 shows the amounts used. For synthesis of nanoparticles separately, same amount of CaCl₂ and Na₂HPO₄ were used as the process described for NP-GelMa synthesis without the methacrylation step.

Each sample was made into a gel by mixing the above materials and putting them in a mold shape and then crosslinking them by irradiating UV light for about 30 minutes. These materials were made in a diameter of 6 mm and a thickness of 2 mm (Figure 1). For synthesis of CNp+GelMa, each crosslinked GelMa and nanoparticles were synthesized separately and mixed together as described above. All samples were carefully manufactured in a sterile laboratory to avoid contamination.

3. Scanning Electron Microscope (SEM) Analysis

The surface properties of GelMa and CNp-GelMa were investigated by Scanning Electron Microscopy (SEM, TESCAN VEGA3, Tescan Korea) at different magnifications under inert environment after drying in – 78 °C lyophilizer and then platinum coating under vacuo for 1 min. The SEM images were uploaded to a computer software (Photoshop CS6; Adobe System, San José, CA, USA) and then observed.

4. Study design

Ten rabbits were used in this study, which were assigned to three groups according to the healing period of 2, 4 and 8 weeks (n=4, 4, and 2, respectively). In each specimen, four

circular defects with a diameter of 6 mm were formed in the calvarium, which were randomly allocated to the following study groups (Figure 2):

- 1) Empty control group
- 2) GelMa group: crosslinked GelMa hydrogel
- 3) CNp-GelMa: crosslinked NP-GelMa hydrogel
- 4) CNp+GelMa: GelMa hydrogel crosslinked and then mixed with calcium phosphate nanoparticles

At two, four and eight weeks, rabbits were sacrificed, and the samples collected for analysis.

5. Sample size determination

The sample size was determined using a specialized tool (G*Power 3.1.9.4, Germany). Calculations were performed based on a previous study using the same experimental model and the primary outcome of the total augmented area (Park et al., 2015). The deduced effect size of 2.4, type I error of 0.05 and the power of 0.80 produced the sample size of $n=4$ for each group at 2 and 4 weeks. Further two animals were allocated for the 8-week group for histologic observation, which were excluded for statistical analysis.

6. Surgical procedure

The surgical procedures were followed in detail based on previous publications (Hong et al., 2020). The surgeries were performed under general anesthesia induced with

inhalation of 2.5% isoflurane and subcutaneous injection of alfaxan (5mg/kg) and medetomidine (0.25mg/kg). The surgical sites were shaved and disinfected with povidone iodine, and infiltration anesthesia was performed using 2% lidocaine with 1: 80,000 epinephrine. The incision was made along the midline of the rabbit calvarium and then a full-thickness flap was elevated. Four circular bone defects were formed using a trephine bur with a diameter of 6mm under saline irrigation without damaging the underlying dura mater or cerebral tissue. These defects were randomly allocated to the control group, GelMa group, CNp-GelMa group and CNp+GelMa group and filled according to the study design. Flap were carefully repositioned and sutured with absorbable 4-0 suture material (4-0 Vicryl, Ethicon, Somerville, NJ, USA).

7. Micro-CT Analysis

All harvested specimens were fixed with 10% formalin for 7 days and scanned with a high-resolution micro-computed tomography system (Sky-Scan 1173, SkyScan, Kartuizersweg 3B 2550 Kontich, Belgium) at a pixel size of 13.93 μm (130 kV, 60 μA). The scanned data sets were processed in Digital Imaging and Communications In Medicine (DICOM) format, and reconstructed with three dimensional (3D) reconstruction software (Nrecon reconstruction program [Ver 1.7.0.4], Bruker-CT, Kontich, Belgium). The region of interest (ROI) was defined by (i) the lateral boundaries of defect sites formed by the trephine bur, (ii) the superiorly; periosteum, (iii) inferiorly; dura mater. The measurements were performed by using an CT analyzing software (CTan [version;1.17.7.2], Bruker micro-CT). Within the region of interest, the following volumes were measured.

- Total augmented volume (TAV; mm^3): Total augmented volume of the ROI, including mineralized tissue, graft material, and fibrovascular connective tissue within the ROI.
- New bone volume (NBV; mm^3): Sum of volumetric measurements of newly-formed bone within the ROI.

8. Histological and histomorphometric analyses

The block samples were decalcified in 5% formic acid for 14 days and embedded in paraffin. Then, 5- μm -thick sections were cut along the middle of each circular defect. Each tissue slide was stained with Hematoxylin-eosin and Masson trichrome staining. The slide images were captured by a digital slide scanner (Panoramic 250 Flash III, 3D HISTECH, Budapest, Hungary). The histomorphometric measurements of defects were performed with a computer-aided slide image analysis program (CaseViewer 2.1, RTM_v2.1.2.69595) and a computer software (Photoshop CS6; Adobe System, San José, CA, USA). The region of interest(ROI) was defined by (i) the lateral boundaries of defect sites formed by the trephine bur, (ii) the superiorly; periosteum, (iii) inferiorly; dura mater. Within the ROI, the following areas were measured.

- Total augmented area (TAA; mm^2): the overall area of new bone, mineralized tissue, graft material, and fibrovascular connective tissue within the ROI.
- New bone area (NBA; mm^2): Sum of areas of newly-formed bone within the ROI.

9. Statistical analysis

The statistical analysis was performed by using a software program (IBM SPSS statistics 26.0; SPSS Chicago, IL, USA). Total augmented volume, new bone volume measurements from micro-CT and total augmented area, new bone area measurements from histomorphometric analysis were summarized by median, mean values and standard deviations. The significance of differences between groups with different materials was determined by the Kruskal-Wallis test followed by the Bonferroni test. The Kruskal-Wallis test was performed for comparisons between different materials within each healing period, and the Mann-Whitney test was used to evaluate the data between each experimental group. Statistical significance was considered at the $P < 0.05$ level.

III. RESULTS

1. Clinical observations

The wound healing was uneventful. None of the sites showed any signs of material exposure or infection throughout the entire study period.

2. Scanning Electron Microscope (SEM) Analysis

The morphological properties of GelMa and CNp-GelMa were shown in Figure 3. The surface of GelMa appeared smooth and homogenous (Figure 3A). In the CNp-GelMa group, spherical nanoparticles were distributed and assimilated throughout the GelMa structure resulting in a rough surface (Figure 3B). Higher magnification (x500; scale bar 100 μ m) showed that nanoparticles of relatively uniform size were evenly spread out and integrated with the hydrogel (Figure 3C).

3. Micro-CT analysis

The results from the statistical analysis are presented in Table 2, Figure 4 and Figure 5. The CNp-GelMa group had the highest TAVs in 2-week and 4-week experimental groups, respectively. The GelMa and CNp-GelMa groups at 8 weeks showed an increase in NBV compared to the corresponding groups at 2 and 4 weeks. At 8 weeks, highest NBV was found in the CNp-GelMa group ($15.34 \pm 3.12 \text{mm}^3$). At both 2 and 8 weeks, the GelMa, CNp-GelMa and CNp+GelMa group showed greater NBV compared the control group. At 4 weeks, the CNp-GelMa and CNp+GelMa group showed greater NBV compared the control group. However, there were no significant differences in NBV and TAV in experimental groups compared to the control group between 2 and 4 weeks.

4. Histologic observations

2 weeks

In control group, little or none of new bone formation was detected at the margin of the defect. Fibrous tissue and brain tissue invaded into the defect area. Inflammatory cells were observed around the margin of the defect (Figure 6A). In GelMa group, most of them were resorbed and some residual materials remained in a few of the samples. Instead, the defect areas were filled with loose connective tissue. However, there were no inflammatory cells surrounding the residual materials (Figure 6B). Likewise, in CNp-GelMa and CNp+GelMa group, small amounts of residual material were observed, and infiltration of inflammatory cells were scarcely detected around the residual material (Figure 6C and 6D). In the high-magnification view, osteoblasts could be observed around the newly formed bone (Figure 6C).

4 weeks

In control group, naturally formed new bone could be found from margin of circular defect to the center. By 4 weeks, woven bone formation originated from the margins of the defect in GelMa group. In CNp-GelMa and CNp+GelMa group, residual materials were completely resorbed, and new bone formation originated from the native bone at the margin of the defect was observed (Figure 7C and 7D).

8 weeks

In GelMa group, immature bone tissues over the defects were visible, which was similar to the natural bone formation in the control group. In CNp-GelMa group, almost complete closure of the defects was achieved (Figure 8C) while in CNp+GelMa group, the defect area was still not fully closed by bone bridge (Figure 8D).

5. Histomorphometric analysis

The results from the histomorphometric analysis are summarized in Table 3 and Figure 9. At 2 weeks, the CNp-GelMa ($4.93 \pm 1.89 \text{ mm}^2$, $p=0.029$) and CNp+GelMa groups ($5.05 \pm 1.11 \text{ mm}^2$, $p=0.029$) showed significantly higher TAA compared to the control group ($2.35 \pm 0.80 \text{ mm}^2$), but there was no significant difference between the GelMa group ($4.00 \pm 1.03 \text{ mm}^2$, $p=0.057$) and the control group. In measurements for NBA, there were no significant differences compared to the control group. At 4 weeks, the CNp-GelMa group exhibited the highest TAA ($6.18 \pm 1.94 \text{ mm}^2$) and the CNp+GelMa group had the highest NBA ($2.68 \pm 0.75 \text{ mm}^2$), however, the differences were not significant.

IV. DISCUSSION

Hydrogels have shown potential as a scaffold for tissue engineering due to its physical characteristic that mimics the extracellular matrix. For bone regeneration, however, it has been typically lacking in stability and space maintenance. The current crosslinked GelMa hydrogel has been developed in combination with nanoceramic particles to enhance these drawbacks. In this study, we evaluated the efficacy of GelMa hydrogels for bone regeneration and compared different methods of fabrication in combination with nanoparticles. The main findings revealed that, (i) in terms of NBV and TAV, greatest bone regeneration was achieved by the CNp-GelMa group at 8 weeks; (ii) GelMa hydrogel combined with nanoparticles were able to remain inside the defect up to 2 weeks; and (iii) the GelMa hydrogel exhibited excellent biocompatibility with low inflammatory response.

In this study, the greatest new bone formation was achieved by the CNp-GelMa group. A close inspection of the histologic representations revealed that there were greater number of sites with complete defect closure in the CNp-GelMa group compared to the other experimental groups. The addition of inorganic nanoparticles to the GelMa hydrogel has been shown to increase the expression of osteogenic genes such as bone sialoprotein, osteocalcin and runt-related transcription factor 2 (Heo et al., 2014a). Furthermore, the nanoparticles were shown to produce other beneficial effects including reinforced structural stability, improved cell proliferation, stimulation of extracellular matrix production, and enhancement of cell-to-cell communication (Mora-Boza and Lopez-Donaire, 2018). The various nano-biomaterials can be classified as ceramics, polymers, carbon, and noble metals. Nanoparticles that we used in this study are calcium phosphate-based materials, which are widely utilized in skeletal tissue engineering as they are the major composition of ECM for strengthening bone regeneration (Trombetta et al., 2017). Although the specific mechanisms are not clear, it is presumed that the nanoparticles added

to GelMa hydrogel can promote new bone formation by mediating cell signaling related to osteoinduction.

The GelMa hydrogel containing nanoparticles could be observed within the defect up to 2 weeks in this study. This was confirmed by the histomorphometric analysis, in which CNp-GelMa and CNp+GelMa groups exhibited greater augmented volume compared to the control group. Notably, the total augmented volume in the GelMa group without the nanoparticles was comparable to that in the control group, which could imply that greater stability might be achieved when GelMa hydrogel is combined with the nanoparticles. Previous studies have shown rapid degradation characteristics of hydrogel derived materials. GelMa hydrogel was completely resorbed by collagenase after 14 days, *in vitro* (Heltmann-Meyer et al., 2021), and polyethylene glycol (PEG) hydrogel was degraded within 10 days *in vitro* (Cha et al., 2018). Rapid resorption of hydrogel was owed to the enzyme-sensitive sequences within its molecular chains which makes it susceptible to degradation by matrix metalloproteinases (MMPs). The results of this study demonstrated that nanoparticles within the crosslinked GelMa hydrogel might behave as a potential stabilizing agent to slow down enzymatic degradation. Nevertheless, the period of stabilization achieved by the addition of nanoparticles in this study was insufficient. This result could be related to early degradation of the GelMa hydrogel or the low concentration of nanoparticles within the hydrogel mixture. In general, the scaffold material should provide space within the defect for at least two months during which early bone formation occurs (Park et al., 2014). In large-sized bone defects in the oral cavity requiring extensive bone regeneration, considerably longer healing periods are advocated, which can vary between six to nine months depending on the defect size (Retzepi and Donos, 2010). In this respect, the mechanical stability and durability of GelMa hydrogel need to be improved. A previous study has shown that the degradation rate of GelMa could be slowed down by increasing the crosslinking density of the methacryloyl group (Zhu et al., 2019). The mechanical properties are affected by the different types and dose of additives, concentration of GelMa as well as the degree of substitution and UV dose (Pepelanova et

al., 2018). In addition, another study reported that the concentration of nanoparticles could be a critical factor to increase stiffness and strength because nanoparticle incorporation in the GelMa hydrogel reinforces its network (Elkhoury et al., 2019). Although the exact interactions between nano-sized particles and hydrogel were not investigated, increase in the content of nanoparticles such as nanoclay or hydroxyapatite (HA) led to increasing trend in stiffness and tensile strength (Xing and Tang, 2021). Moreover, it was revealed that different strategies of incorporation of nanoparticles could improve fragile property of GelMa. Both physical and covalent integration of nanoparticles into GelMa hydrogel could achieve mechanical advantages and in certain cases, nanoparticles acted as physical fillers in the hydrogel network, ensuring higher mechanical strength and toughness irrespective of its mode of synthesis (Dannert et al., 2019). Accordingly, the current outcomes indicate that such measures need to be taken further in future studies to improve the mechanical stability of GelMa hydrogel.

In this study, two different manufacturing methods were used to prepare nanoparticles reinforced GelMa hydrogel. The CNp-GelMa was prepared by one pot synthesize technique, which means GelMa and the nanoparticles were chemically crosslinked, whereas the CNp+GelMa was simply a mixture of the nanoparticles and GelMa that have been separately crosslinked. According to previous studies, the chemical crosslinking of nanoparticles to GelMa hydrogel enhanced the mechanical stiffness and resistance to enzymatic degradation (Dong et al., 2019; Zhang et al., 2021). Histologically, remnants of CNp-GelMa and CNp+GelMa were observed at 2 weeks, but they were not maintained at 4 weeks. Therefore, these materials need to be improved in terms of stiffness and stability, and further study should be performed to find the optimal crosslinking method.

In histologic analysis, minimal inflammatory reactions were observed in the experimental groups containing GelMa and the nanoparticles, which indicates that GelMa has good biocompatibility. It has been shown in previous studies that such good biocompatibility is exhibited by hydrogels in general (Heltmann-Meyer et al., 2021).

Biocompatibility is an essential characteristic of any biomaterial and is one of the main reasons why GelMa hydrogel has been considered for bone tissue engineering.

Another advantage of GelMa hydrogel is that it can be produced by three-dimensional bioprinting. Since the chemical, physical and mechanical characteristics of GelMa hydrogel can be easily modified by manipulating its components, it is feasible to fabricate cell-laden materials to mimic the structure of native tissues. Also, during the printing process, construction of hybrid hydrogels can be conjugated with various nanofillers suitable for the target tissue (Modaresifar et al., 2018; Yue et al., 2015). In that respect, GelMa hydrogel is a promising material for expanding spectrum of applications in many other biomedicines.

8mm circular defect in rabbit calvarial model is generally used in assessing the effects of bone graft materials (Hong et al., 2020). However, for the present study, the diameter of the defects was 6 mm. Although 6 mm is smaller than the critical size indicated in the literature, a smaller dimension has been recommended to evaluate shorter healing period (Sohn et al., 2010). In addition, a healing period of 2 and 4 weeks was chosen to observe the early healing response while a healing period of 8 weeks was chosen to assess the late healing at which the extent of defect regeneration can be observed (Sohn et al., 2010).

The limitation in this study was the lack of in vitro experiments to evaluate material characteristics such as cytotoxicity, various mechanical strength tests and degradation kinetics. Further in vitro tests on degradation rate should be performed prior to in vivo application in future studies since this material has shown good biocompatibility and promising potentials as a scaffold for tissue engineering.

V. CONCLUSION

In summary, there was no difference in the efficacy of bone regeneration according to the synthesized method of photo-crosslinked GelMa hydrogel with nanoparticles. However, these materials could remain within a bone defect up to 2 weeks and showed good biocompatibility with little inflammatory response. Further studies should aim to enhance the mechanical properties and resistance to enzymatic degradation prior to application in bone regenerative procedures.

REFERENCE

- Annabi N, Nichol JW, Zhong X, Ji C, Koshy S, Khademhosseini A, et al. (2010). Controlling the porosity and microarchitecture of hydrogels for tissue engineering. *Tissue Eng Part B Rev* 16(4): 371-383.
- Bhattacharyya A, Janarthanan G, Kim T, Taheri S, Shin J, Kim J, et al. (2022). Modulation of bioactive calcium phosphate micro/nanoparticle size and shape during in situ synthesis of photo-crosslinkable gelatin methacryloyl based nanocomposite hydrogels for 3D bioprinting and tissue engineering. *Biomater Res* 26(1): 54.
- Cha JK, Jung UW, Thoma DS, Hammerle CHF, Jung RE (2018). Osteogenic efficacy of BMP-2 mixed with hydrogel and bone substitute in peri-implant dehiscence defects in dogs: 16 weeks of healing. *Clin Oral Implants Res* 29(3): 300-308.
- Dannert C, Stokke BT, Dias RS (2019). Nanoparticle-Hydrogel Composites: From Molecular Interactions to Macroscopic Behavior. *Polymers* 11(2).
- Dong ZQ, Yuan QJ, Huang KQ, Xu WL, Liu GT, Gu ZP (2019). Gelatin methacryloyl (GelMA)-based biomaterials for bone regeneration. *Rsc Advances* 9(31): 17737-17744.
- Elkhoury K, Russell CS, Sanchez-Gonzalez L, Mostafavi A, Williams TJ, Kahn C, et al. (2019). Soft-Nanoparticle Functionalization of Natural Hydrogels for Tissue Engineering Applications. *Adv Healthc Mater* 8(18): e1900506.
- Heltmann-Meyer S, Steiner D, Muller C, Schneidereit D, Friedrich O, Salehi S, et al. (2021). Gelatin methacryloyl is a slow degrading material allowing vascularization and long-term use in vivo. *Biomedical Materials* 16(6).

- Heo DN, Ko WK, Bae MS, Lee JB, Lee DW, Byun W, et al. (2014a). Enhanced bone regeneration with a gold nanoparticle-hydrogel complex. *J Mater Chem B* 2(11): 1584-1593.
- Heo DN, Ko WK, Bae MS, Lee JB, Lee DW, Byun W, et al. (2014b). Enhanced bone regeneration with a gold nanoparticle-hydrogel complex. *Journal of Materials Chemistry B* 2(11): 1584-1593.
- Hong I, Khalid AW, Pae HC, Cha JK, Lee JS, Paik JW, et al. (2020). Distinctive bone regeneration of calvarial defects using biphasic calcium phosphate supplemented ultraviolet-crosslinked collagen membrane. *Journal of Periodontal and Implant Science* 50(1): 14-27.
- Jiao Y, Li C, Liu L, Wang F, Liu X, Mao J, et al. (2020). Construction and application of textile-based tissue engineering scaffolds: a review. *Biomater Sci* 8(13): 3574-3600.
- Lee KY, Mooney DJ (2001). Hydrogels for tissue engineering. *Chemical Reviews* 101(7): 1869-1879.
- Li Y, Rodrigues J, Tomas H (2012). Injectable and biodegradable hydrogels: gelation, biodegradation and biomedical applications. *Chem Soc Rev* 41(6): 2193-2221.
- Liu Y, Chan-Park MB (2010). A biomimetic hydrogel based on methacrylated dextran-graft-lysine and gelatin for 3D smooth muscle cell culture. *Biomaterials* 31(6): 1158-1170.
- McBeth C, Lauer J, Ottersbach M, Campbell J, Sharon A, Sauer-Budge AF (2017). 3D bioprinting of GelMA scaffolds triggers mineral deposition by primary human osteoblasts. *Biofabrication* 9(1): 015009.

- Modaresifar K, Hadjizadeh A, Niknejad H (2018). Design and fabrication of GelMA/chitosan nanoparticles composite hydrogel for angiogenic growth factor delivery. *Artif Cells Nanomed Biotechnol* 46(8): 1799-1808.
- Mora-Boza A, Lopez-Donaire ML (2018). Preparation of Polymeric and Composite Scaffolds by 3D Bioprinting. *Adv Exp Med Biol* 1058: 221-245.
- Noh I, Kim N, Tran HN, Lee J, Lee C (2019). 3D printable hyaluronic acid-based hydrogel for its potential application as a bioink in tissue engineering. *Biomater Res* 23: 3.
- Park JI, Yang C, Kim YT, Kim MS, Lee JS, Choi SH, et al. (2014). Space maintenance using crosslinked collagenated porcine bone grafted without a barrier membrane in one-wall intrabony defects. *Journal of Biomedical Materials Research Part B-Applied Biomaterials* 102(7): 1454-1461.
- Park JY, Yang C, Jung IH, Lim HC, Lee JS, Jung UW, et al. (2015). Regeneration of rabbit calvarial defects using cells-implanted nano-hydroxyapatite coated silk scaffolds. *Biomater Res* 19: 7.
- Pepelanova I, Kruppa K, Scheper T, Lavrentieva A (2018). Gelatin-Methacryloyl (GelMA) Hydrogels with Defined Degree of Functionalization as a Versatile Toolkit for 3D Cell Culture and Extrusion Bioprinting. *Bioengineering (Basel)* 5(3).
- Rahali K, Ben Messaoud G, Kahn CJF, Sanchez-Gonzalez L, Kaci M, Cleymand F, et al. (2017). Synthesis and Characterization of Nanofunctionalized Gelatin Methacrylate Hydrogels. *Int J Mol Sci* 18(12).
- Retzepe M, Donos N (2010). Guided Bone Regeneration: biological principle and therapeutic applications. *Clin Oral Implants Res* 21(6): 567-576.
- Serafim A, Tucureanu C, Petre DG, Dragusin DM, Salageanu A, Van Vlierberghe S, et al. (2014). One-pot synthesis of superabsorbent hybrid hydrogels based on

- methacrylamide gelatin and polyacrylamide. Effortless control of hydrogel properties through composition design. *New Journal of Chemistry* 38(7): 3112-3126.
- Sohn JY, Park JC, Um YJ, Jung UW, Kim CS, Cho KS, et al. (2010). Spontaneous healing capacity of rabbit cranial defects of various sizes. *J Periodontal Implant Sci* 40(4): 180-187.
- Trombetta R, Inzana JA, Schwarz EM, Kates SL, Awad HA (2017). 3D Printing of Calcium Phosphate Ceramics for Bone Tissue Engineering and Drug Delivery. *Ann Biomed Eng* 45(1): 23-44.
- Van Den Bulcke AI, Bogdanov B, De Rooze N, Schacht EH, Cornelissen M, Berghmans H (2000). Structural and rheological properties of methacrylamide modified gelatin hydrogels. *Biomacromolecules* 1(1): 31-38.
- Wang N, Ma M, Luo Y, Liu TZ, Zhou P, Qi SC, et al. (2018). Mesoporous Silica Nanoparticles-Reinforced Hydrogel Scaffold together with Pinacidil Loading to Improve Stem Cell Adhesion. *Chemnanomat* 4(7): 631-641.
- Xiao S, Zhao T, Wang J, Wang C, Du J, Ying L, et al. (2019). Gelatin Methacrylate (GelMA)-Based Hydrogels for Cell Transplantation: an Effective Strategy for Tissue Engineering. *Stem Cell Rev Rep* 15(5): 664-679.
- Xing W, Tang Y (2021). On mechanical properties of nanocomposite hydrogels: Searching for superior properties. *Nano Materials Science*.
- Yue K, Trujillo-de Santiago G, Alvarez MM, Tamayol A, Annabi N, Khademhosseini A (2015). Synthesis, properties, and biomedical applications of gelatin methacryloyl (GelMA) hydrogels. *Biomaterials* 73: 254-271.

Zhang Y, Sun M, Liu T, Hou M, Yang H (2021). Effect of Different Additives on the Mechanical Properties of Gelatin Methacryloyl Hydrogel: A Meta-analysis. *ACS Omega* 6(13): 9112-9128.

Zhu M, Wang Y, Ferracci G, Zheng J, Cho NJ, Lee BH (2019). Gelatin methacryloyl and its hydrogels with an exceptional degree of controllability and batch-to-batch consistency. *Sci Rep* 9(1): 6863.

TABLES

Table 1. The composition of different GelMa hydrogel samples.

GelMa			CNp-GelMa			CNp+GelMa			CNp		
GelMa 0.4g	Gelatin	1g	GelMa 0.4g	Gelatin	1g	GelMa 0.4g	Gelatin	1g	CNp 0.4g	CaCl ₂	0.11g
	7.4 PBS	100ml		Na ₂ HPO ₄	0.0852g		7.4 PBS	100ml		Na ₂ HPO ₄	0.0852g
	Metacrylic Anhydride	4ml		Metacrylic Anhydride	4ml		Metacrylic Anhydride	4ml		7.4 PBS	50ml
				7.4 PBS	50ml					D.W	50ml
				D.W	50ml						
	Irgacure	40mg		Irgacure	40mg		Irgacure	40mg		Irgacure	40mg
	D.W	1ml		D.W	1ml		D.W	1ml		D.W	1ml
							CNp	70mg			

Table 2. Volumetric results from the micro-CT analysis (mm³).

Healing Period	Study Group	Total augmented volume		New bone volume	
		Median	Mean±SD	Median	Mean±SD
2 weeks (n=4)	Control	71.37	74.41±13.01	1.80	4.66±6.29
	GelMa	66.65	69.70±7.69	9.81	8.87±3.04
	CNp-GelMa	79.43	77.66±12.56	7.92	8.28±1.42
	CNp+GelMa	69.79	74.91±18.80	6.09	6.36±2.28
4 weeks (n=4)	Control	65.08	65.27±3.97	8.60	9.64±7.46
	GelMa	64.88	66.06±7.57	7.07	7.50±5.96
	CNp-GelMa	70.19	70.29±6.70	14.23	13.49±7.84
	CNp+GelMa	69.20	70.19±5.80	14.25	14.50±3.07
8 weeks (n=2)	Control	85.52	85.52±30.31	2.25	2.25±2.22
	GelMa	74.91	74.91±0.83	13.95	13.95±14.09
	CNp-GelMa	68.22	68.22±6.40	15.34	15.34±3.12
	CNp+GelMa	75.10	75.10±21.13	8.95	8.95±2.12

*Significantly different to the control group (p<0.05)

Table 3. Results from the histomorphometric analysis (mm²).

Healing Period	Study Group	Total augmented area		New bone area	
		Median	Mean±SD	Median	Mean±SD
2 weeks (n=4)	Control	2.23	2.35±0.80	0.64	0.90±0.70
	GelMa	3.83	4.00±1.03	1.13	1.20±0.32
	CNp-GelMa	4.32	*4.93±1.89	1.76	2.02±1.19
	CNp+GelMa	4.57	*5.05±1.11	1.59	1.49±0.52
4 weeks (n=4)	Control	4.11	4.00±1.57	1.57	1.71±1.26
	GelMa	4.81	4.47±1.71	1.49	1.45±0.93
	CNp-GelMa	5.81	6.18±1.94	2.11	2.67±1.72
	CNp+GelMa	6.14	5.73±1.20	2.94	2.68±0.75
8 weeks (n=2)	Control	2.20	2.20±0.14	0.73	0.73±0.31
	GelMa	6.55	6.55±5.80	2.97	2.97±3.50
	CNp-GelMa	6.11	6.11±2.89	3.25	3.25±1.41
	CNp+GelMa	4.96	4.96±0.78	2.22	2.22±1.63

*Significantly different to the control group (p<0.05)

FIGURES



Figure 1. Clinical photograph of surgical intervention.

(A) Sample 1: Crosslinked GelMa hydrogel (GelMa) (B) Sample 2: Crosslinked in situ calcium phosphate nanoparticles and GelMa (CNp-GelMa) (C) Sample 3: Crosslinked GelMa + calcium phosphate nanoparticles mixed (CNp+GelMa)

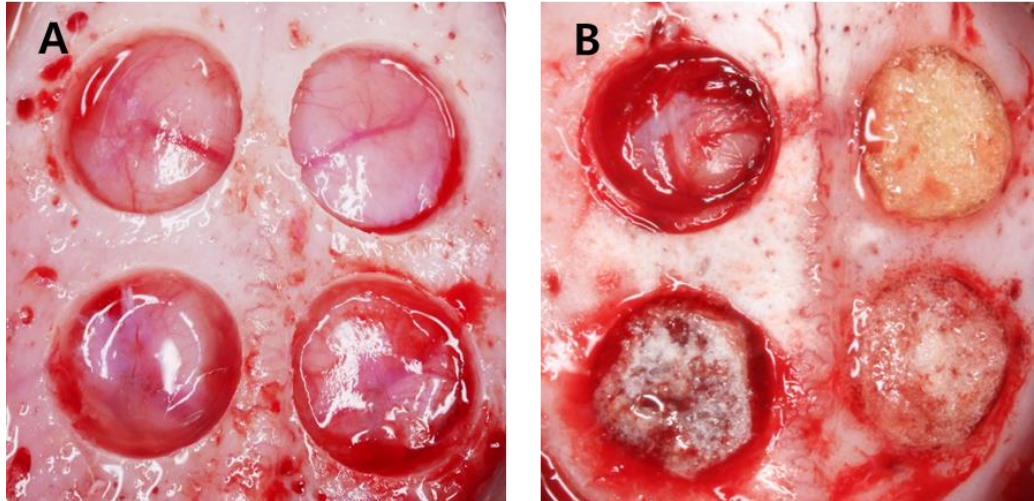


Figure 2. Experimental design in the rabbit calvarium.

(A) Four 6mm diameter defects were made in each calvaria of rabbits using a trephine bur.

(B) Each defect was randomly assigned to an experimental group and filled with different materials. Clockwise from top left; Control group(unfilled), Sample 1: GelMa, Sample 2: CNp-GelMa, Sample 3: CNp +GelMa

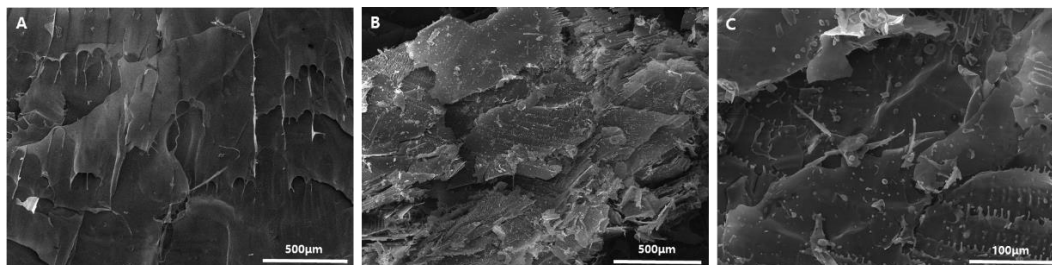


Figure 3. Microstructure surface images of samples using scanning electron microscopy (15.0 kV).

(A) Crosslinked GelMa hydrogel exhibiting a smooth surface (x100 magnification). (B) Crosslinked in situ calcium phosphate nanoparticles and GelMa (CNp-GelMa) showing spherical nanoparticles distributed throughout the hydrogel structure (x100 magnification). (C) Crosslinked in situ calcium phosphate nanoparticles and GelMa (CNp-GelMa) showing integration of the nano particles on the surface of the hydrogel (x500 magnification).

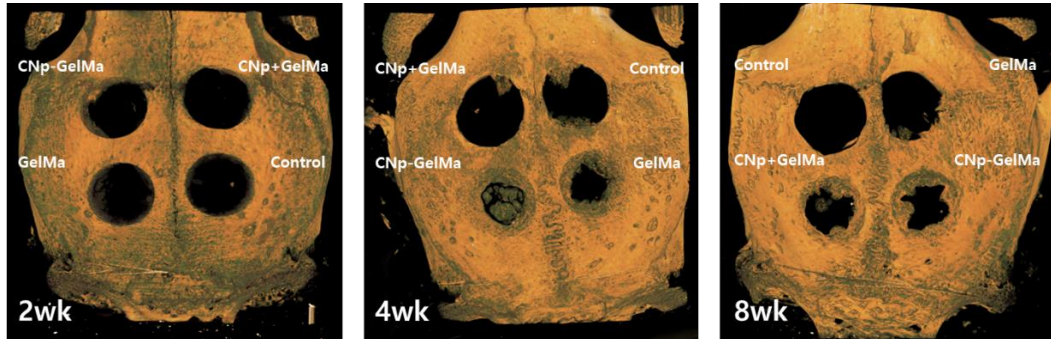


Figure 4. Three-dimensionally reconstructed micro-computed tomography images of the rabbit calvaria at 2, 4 and 8 weeks.

It can be seen that bone formation was more pronounced in the groups containing the GelMa hydrogel.

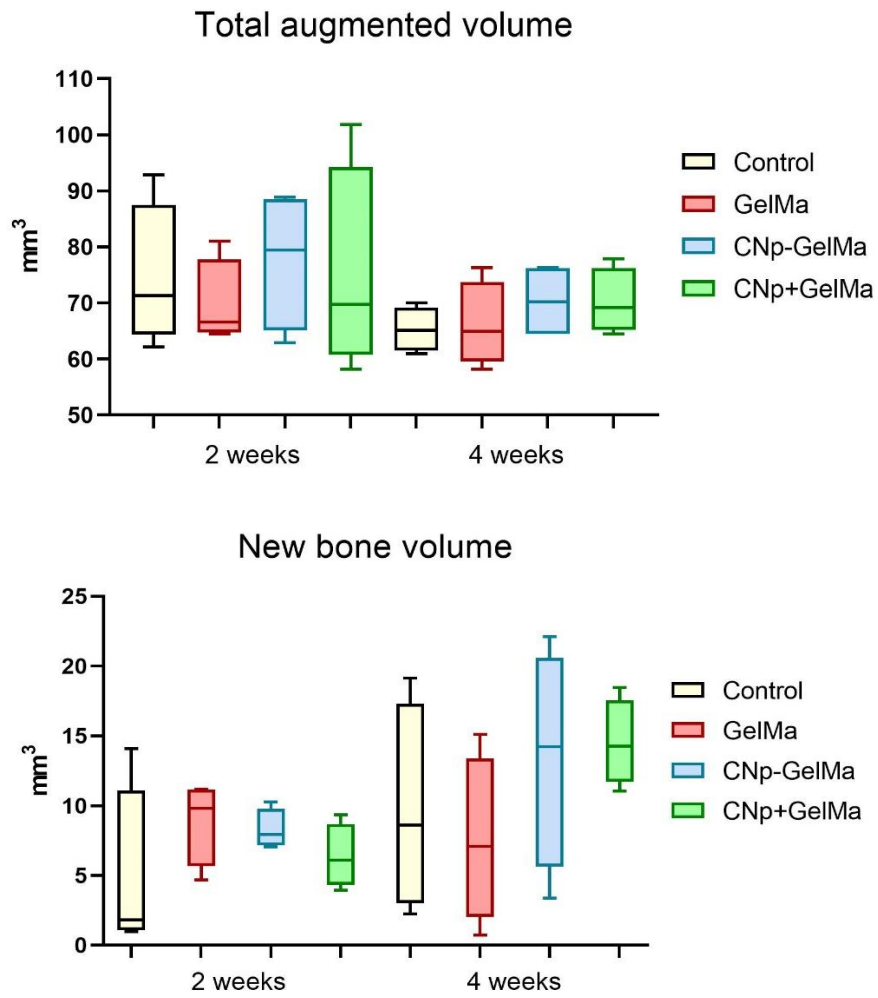


Figure 5. The results from the volumetric analysis represented as graphs.

*Significantly different to the control group ($p < 0.05$)

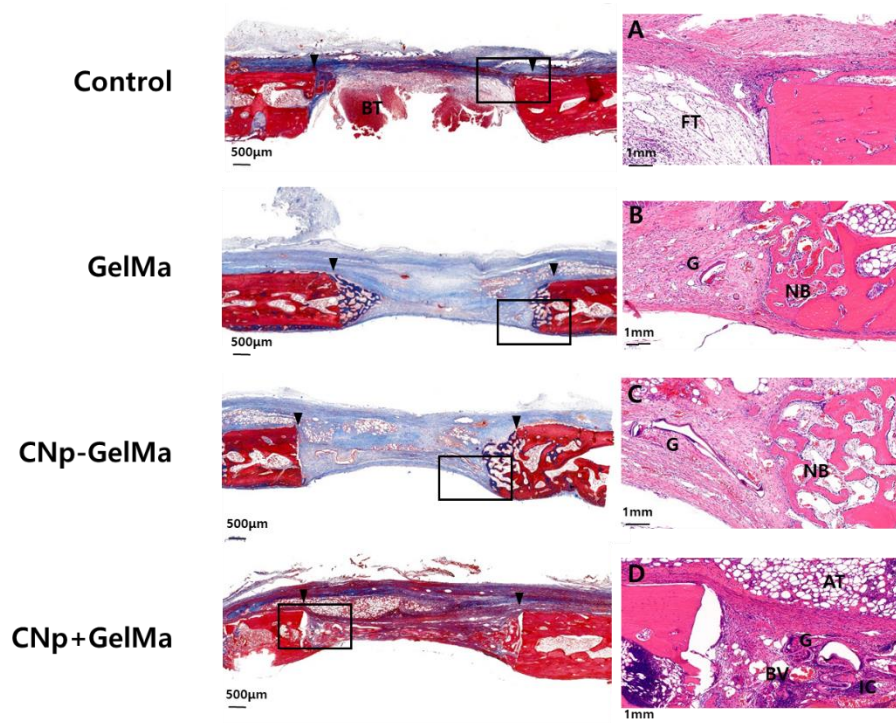


Figure 6. Histological view of each group at 2 weeks.

(A) The control group. (B) The GelMa group: crosslinked GelMa hydrogel. (C) The CNp-GelMa group: GelMa hydrogel mixed with nanoparticles and crosslinked. (D) The CNp+GelMa group: GelMa hydrogel crosslinked and then mixed with nanoparticles. The applied materials remained partially over the defect area. A minimal inflammatory reaction occurred around GelMa hydrogel residues. The boxes areas in the left panels (magnification x 2, Masson trichrome stain) are magnified in the corresponding panels on the right (magnification x 10, H-E stain). The defect margin is labeled with an arrowhead. BT: brain tissue, NB: new bone, FT: fibrous tissue, AT: adipose tissue, IC: inflammatory cells, BV: blood vessel, G: residual materials.

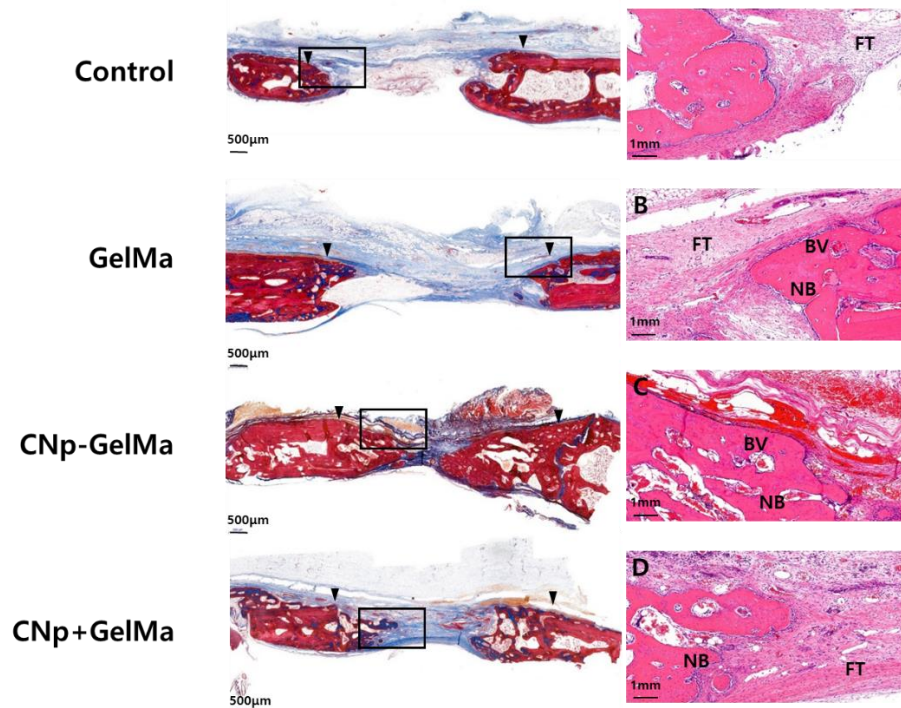


Figure 7. Histological view of each group at 4 weeks.

(A) The control group. (B) The GelMa group: crosslinked GelMa hydrogel. (C) The CNp-GelMa group: GelMa hydrogel mixed with nanoparticles and crosslinked. (D) The CNp+GelMa group: GelMa hydrogel crosslinked and then mixed with nanoparticles. The inflammatory response subsided and new bone growth into the defect area were observed, especially in CNp-GelMa group. The boxes areas in the left panels (magnification x 2, Masson trichrome stain) are magnified in the corresponding panels on the right (magnification x 10, H-E stain). The defect margin is labeled with an arrowhead. NB: new bone, FT: fibrous tissue, BV: blood vessel.

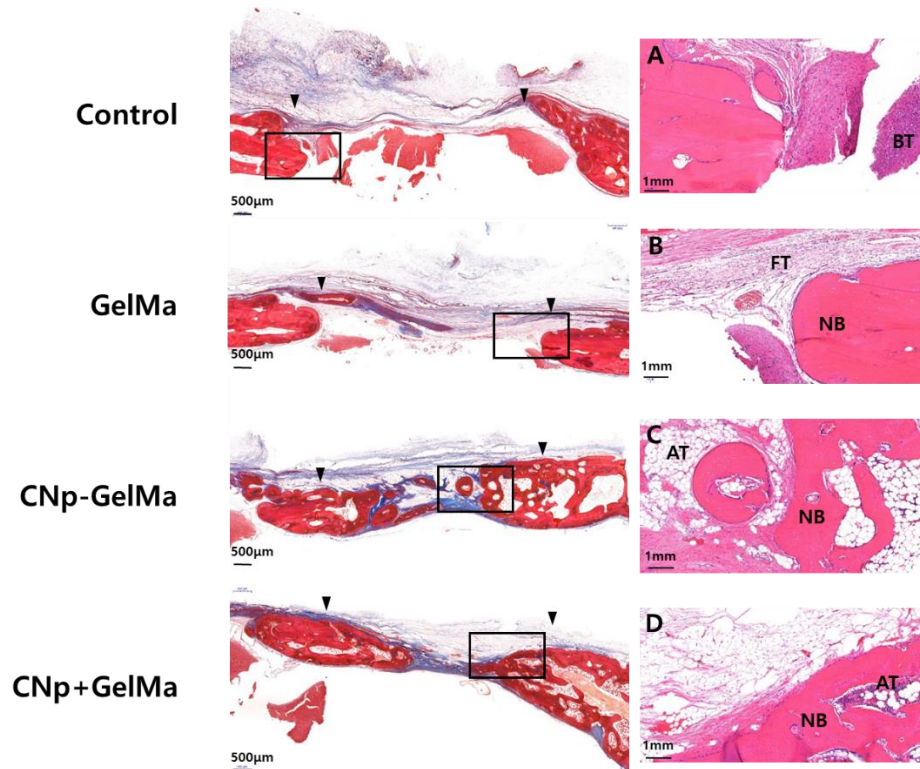


Figure 8. Histological view of each group at 8 weeks.

(A) The control group, (B) The GelMa group: crosslinked GelMa hydrogel. (C) The CNp-GelMa group: GelMa hydrogel mixed with nanoparticles and crosslinked. (D) The CNp+GelMa group: GelMa hydrogel crosslinked and then mixed with nanoparticles. Almost complete closure of the defects was observed in the CNp-GelMa group. The boxes areas in the left panels (magnification x 2, Masson trichrome stain) are magnified in the corresponding panels on the right (magnification x 10, H-E stain). The defect margin is labeled with an arrowhead. BT: brain tissue, NB: new bone, FT: fibrous tissue, AT: adipose tissue.

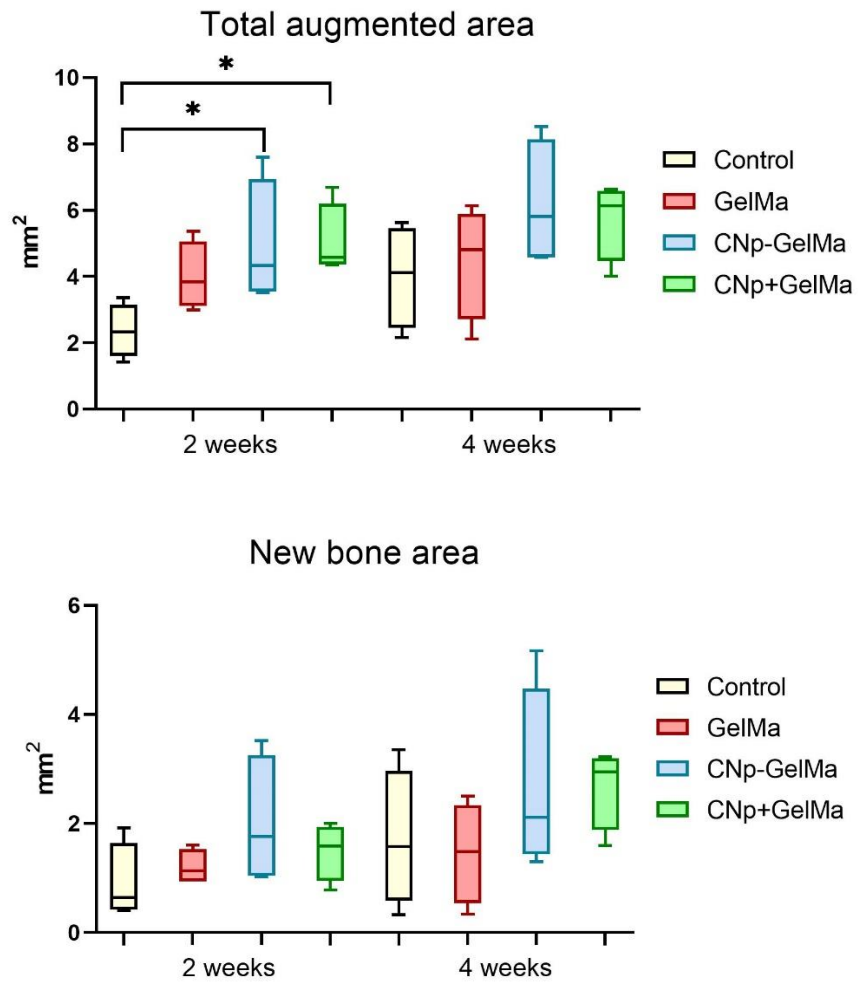


Figure 9. The results from the histomorphometric analysis represented as bar charts.

*Significantly different to the control group ($p < 0.05$)

국문요약

토끼 두개골 결손부에서 나노입자로 강화된 광경화성 Gelatin methacryloyl hydrogel 골재생

<지도교수 최 성 호>

연세대학교 대학원 치의학과

이 다 나

조직 공학에서 스캐폴드의 역할은 재생 과정에서 손상된 조직을 일시적으로 대체하는 것이다. 스캐폴드의 이상적인 특성으로서 세포증식 및 기능적 분화를 위한 환경 제공할 수 있어야하고, 기계적 지지를 필요로 한다. 현재까지 다양한 형태의 생체 재료가 세포조직과 세포활동을 조절하고, 대사물질 및 성장인자를 분배할 수 있는 세포외기질(extracellular matrix, ECM)의 역할을 모방하기 위해 조직 공학 분야에서 연구되고, 개발되고 있다.

하이드로겔(hydrogel)은 세포외기질과 유사한 특성을 가진 스캐폴드로서 다양하게 연구되고 있다. 하이드로겔은 삼차원적 구조의 친수성기를 포함하는 생체물질로 합성고분자와 천연고분자로 제조될 수 있다. 합성고분자는 분해속도 및 기계적 물성을 조절할 수 있는 장점을 지니고, 천연고분자는 세포신호 조절 및 생분해능의 특성을 가지지만, 기계적 물성이 약하다는 단점을 지닌다. 따라서 이 두 물질의 장점을 이용하려는 연구들이 행해지고 있다.

최근, Gelatin methacryloyl(GelMa)는 바이오프린팅과 바이오제조 분야에서 다양하게 이용될 수 있는 생체물질로 주목받고 있으며, 여러 물질을

첨가함으로써 기계적인 물성과 분해 속도를 조절할 수 있는 특징을 가진다. 이러한 첨가물이 GelMa 하이드로겔의 기계적 물성을 개선시킬 수 있는지에 대해서는 여전히 논란의 여지가 있으나, 여러 연구들에서 실질적인 적용을 위한 개발이 시도되고 있다. 탄소 나노튜브와 산화 그래핀을 첨가한 연구에서는 이 재료들의 첨가가 GelMa 하이드로겔의 강성을 높이는 데 효과적임이 입증되었다. 또한 다른 연구에서는 금속 나노입자를 첨가했을 때 신생골 형성에서 유의미한 결과를 얻었다고 보고되었다. 이러한 선행연구에서 착안하여 본 연구에서는 인산칼슘을 기반으로 한 나노입자를 개발하였고, 이와 함께 합성한 GelMa 하이드로겔을 생체 내 모델에 처음으로 적용하여 이 재료가 골 재생을 향상시킬 것이라는 가설을 수립하였다.

따라서 본 연구는 나노입자로 강화된 GelMa 하이드로겔의 골재생 효능을 연구하는 데에 목적을 두었으며, GelMa 하이드로겔에 나노입자를 첨가하는 제조 방식의 차이에 따른 골재생능과 생체적합성 및 분해 양상을 평가할 것이다.

총 10 마리의 각 토끼 두개골에 직경 6mm 의 구형 결손부 4 개를 형성하였다. 각 결손부는 4 개의 군으로 무작위로 할당되었으며, 첫번째 군은 아무 재료도 넣지 않은 대조군 (control group), 두번째 군은 가교결합된 GelMa 하이드로겔을 적용한 군 (GelMa group), 세번째는 나노입자와 GelMa 하이드로겔을 가교결합한 군 (CNp-GelMa group), 네번째는 나노입자와 GelMa 하이드로겔을 각각 합성한 뒤에 이를 혼합한 군 (CNp+GelMa group)으로 설정하였다. 결손부에 각 실험 재료를 적용하고, 2 주에 4 마리, 4 주에 4 마리, 8 주에 2 마리를 희생하였으며, 조직학적 분석과 방사선학적 분석을 통해 4 개 군의 결과를 비교하였다. 방사선학적으로 관심영역 (ROI)을 trephine bur 로 형성한 주변 경계를 기준으로 상부는 골막, 하연은 경막으로 설정하고, 분석 프로그램을 이용하여 전체 증강된 부피 (TAV, mm³)와 신생골

부피 (NBV, mm³)를 측정하였다. 조직학적으로는 광학 현미경을 통한 고배율 관찰과 더불어, 관심영역 (ROI) 내 전체 증강된 면적 (TAA, mm²)과 신생골 면적 (NBA, mm²)을 측정하였다. 조직학적 및 방사선학적 측정치의 통계적 비교는 각 치유 기간에 따른 비교를 위해 Kruskal-Wallis 검정을 시행하였고, 각 실험군 간의 비교는 Mann-Whitney 검정을 시행하였다($p < 0.05$).

임상적으로 양호한 치유 양상을 보였고, 실험 기간 동안 재료의 노출이나 감염으로 인한 염증반응은 보이지 않았다. 방사선학적 측정 결과, 신생골 부피 비교시 8 주에서 CNp-GelMa 군에서 신생골이 가장 많이 형성됨을 확인하였으나 통계적으로 유의미한 차이는 없었다. 조직학적 관찰 결과에서도 CNp-GelMa 군에서 가장 많은 신생골이 관찰되었으나, 면적 측정 결과에서는 통계적으로 유의미한 차이를 보이지 않았다. 2 주에서 대조군과 비교했을 때 CNp-GelMa 군 (4.93 ± 1.89 mm², $p = 0.029$)과 CNp+GelMa 군 (5.05 ± 1.11 mm², $p = 0.029$)이 전체 증강된 면적에서 통계적으로 유의하게 더 큰 값을 확인할 수 있었다. 신생골의 면적은 모든 치유기간동안 대조군과 비교했을 때 유의미한 결과를 얻지 못했다.

결론적으로, 나노입자로 강화된 GelMa 하이드로겔의 제조 방식에 따른 골재생 효능은 차이가 없었다. 하지만, GelMa 하이드로겔과 비교했을 때 나노입자를 첨가한 GelMa 하이드로겔은 2 주까지 결손부 내에 남아있었고, 거의 염증반응 없이 우수한 생체적합성을 보였다. 따라서 임상에 적용하기 위해서는 후속연구를 통해 재료의 기계적인 물성과 효소 분해에 대한 저항성을 개선해야 할 것이다.

핵심되는 말: 동물실험, 생체재료, 골재생, gelatin methacryloyl, 나노입자